AN ANALYSIS OF THE MSRE U-233 INITIAL CRITICALITY FOR BENCHMARK PROBLEM DEVELOPMENT

A Dissertation
Presented to
The Academic Faculty

by

Paul Burke

In Partial Fulfillment
of the Requirements for the Degree
Master's in Nuclear Engineering in the
George W. Woodruff School of Mechanical Engineering

Georgia Institute of Technology
December 2019

AN ANALYSIS OF THE MSRE U-233 INITIAL CRITICALITY FOR BENCHMARK PROBLEM DEVELOPMENT

Approved by:

Dr. Farzad Rahnema, Advisor
School of Mechanical Engineering
Georgia Institute of Technology

Dr. Bojan Petrovic
School of Mechanical Engineering
Georgia Institute of Technology

Dr. Massimiliano Fratoni
College of Engineering
University of California, Berkeley

Date Approved: December 2, 2019

ACKNOWLEDGEMENTS

This research was performed using funding received from the DOE Office of Nuclear Energy's Nuclear Energy University Program. This research was also performed under appointment to the Rickover Fellowship Program in Nuclear Engineering sponsored by the Naval Reactors Division of the U.S. Department of Energy.

I would also like to acknowledge the support of all the faculty in the Department of Nuclear and Radiological Engineering who have helped me since joining the department as an undergraduate, as well as all my family and friends who have helped me along the way.

TABLE OF CONTENTS

LIST OF TABLES

LIST OF FIGURES

LIST OF SYMBOLS AND ABBREVIATIONS

EFPH	Effective Full-Power Hours
°F	Degree Fahrenheit
FHR	Fluoride-Salt-Cooled High-Temperature Reactor
FLiBe	(LiF-BeF_2-ZrF_4-UF_4)
$ft.^3$	Cubic Foot
$^{\delta k}/_{k}$	Reactivity
k_{eff}	Criticality Eigenvalue
kg	Kilogram
MSR	Molten Salt Reactor
MSRE	Molten Salt Reactor Experiment
MW_{th}	Megawatt, Thermal
ORNL	Oak Ridge National Laboratory
pcm	Percent-milli, or 10^{-5}

SUMMARY

The Molten Salt Reactor Experiment (MSRE) was a demonstration molten salt reactor (MSR) operated at Oak Ridge National Laboratory in the 1960's. The reactor was operated in two phases: one with ^{235}U-based fuel salt, and one with ^{233}U-based fuel salt. This work assesses the feasibility of using experimental data from the ^{233}U zero-power initial critical experiment for the development of a criticality benchmark problem. This includes a reconstruction of best-estimate values for several key model inputs (including reactor geometry elements, experimental conditions, and material composition), as well as an initial uncertainty analysis to quantify the standard uncertainty that could be expected for an associated benchmark description.

A set of dominating gaps and experimental uncertainties, including reactor geometry and material properties, were evaluated using an MCNP 6.1 model of the experiment. Some of these gaps are derived effects due to previous operation of the reactor, while others are due to fundamental reported data. The following elements were analyzed for their contribution to standard uncertainty:

- Reactor vessel geometry
- Control rod position
- Sample basket and contents
- Salt composition
- Graphite density
- Isotopic modifications due to previous power operation

These elements were calculated to contribute 570 ± 28 pcm of standard uncertainty in k_{eff}. An additional set of factors were noted but not analyzed due to their expected low contribution to the standard uncertainty. These factors combined are expected to contribute no more than an additional 50 pcm. The most dominant factors were determined to be the density of the graphite moderator, the initial lithium isotopic composition in the fuel salt, and the density of uranium in the fuel salt. The final k_{eff} of the experiment model was calculated to be 1.00957 ± 0.00006.

Additionally, there is an additional reactivity effect predicted by the experimenters due to the presence of low cross section fission products in the salt at the time of the experiment. Predicted to be less than 500 pcm in magnitude, this effect was not analyzed due to a lack of sufficient data in order to recreate the effect. As such, since this negative reactivity effect is not captured in the model, this is best presented as a positive model bias.

It is concluded that, although this uncertainty would generally be considered unacceptable for the purposes of benchmark experimental description development, the lack of experimental data surrounding the use of MSR materials in reactor physics experiments means that readers may still find the experiment useful for benchmarking tools for MSR applications, at least until such time as new experiments become available.

CHAPTER 1. INTRODUCTION

Recent industry research in advanced reactor technology has led to renewed interest in molten salt reactor (MSR) concepts. MSRs are characterized by a liquid fuel salt circulating in the core, which brings a host of reactor physics and safety benefits. A related concept is the Fluoride Salt-Cooled High Temperature Reactor (FHR). This concept involves a solid fuel form with a liquid salt coolant. The two concepts are similar in that they often use similar salts, structural materials, and moderators. In addition, the two concepts are also similar in that they share a lack of validated experimental data for use in benchmarking neutronic simulation codes.

To validate simulation tools for use in reactor design, it is desired to test those tools against a suite of validated benchmark problems. These benchmark problems are based on experimental data, for the purpose of comparing the solution obtained by tools against a known experimental result. For criticality benchmark problems, the target solution is typically an experimentally observed criticality eigenvalue (k_{eff}) of 1. In constructing these benchmark problems, an accurate quantification of the associated experimental uncertainty and statistical biases is crucial.

In the field of MSRs and FHRs, there is an extreme lack of experimental reactor physics data upon which to draw for the purposes of benchmark development. It is thus of utmost importance to make the best use of the experimental data that is available in the field. This is the underlying reasoning behind this work, which examines an experiment from the operation of the Molten Salt Reactor Experiment (MSRE), a demonstration MSR operated at Oak Ridge National Laboratory (ORNL) in the 1960s.

The MSRE was a 10 MW_{th} (as designed, operated power was slightly less) graphite-moderated MSR with FLiBe ($LiF\text{-}BeF_2\text{-}ZrF_4\text{-}UF_4$) fuel salt. It operated for several years, accruing about 13,000 effective full-power hours (EFPH) of operation. The first 9,000 EFPH were run with fuel salt comprising primarily uranium-235 (^{235}U). After this first phase of operation, the uranium was cleaned from the salt, and the clean salt was re-loaded with stock comprising primarily ^{233}U. A set of experiments were performed with this ^{233}U fuel salt, including an initial critical experiment. The focus of this work is examining the experimental data surrounding this ^{233}U critical experiment. This work is a discussion of the process of bringing together data from different sets of available documentation in order to reconstruct best-estimate values for modeling data. Additionally, uncertainty in the experimental data and its effect on the criticality will be assessed, culminating in an estimate of the overall experimental uncertainty in criticality. First, an overview of the reactor will be presented, as well as relevant experimental data. A set of modeling difficulties, uncertainties, and gaps in information will be presented, along with their effect on the criticality of the model. With these results, a short discussion about the implication of the magnitude of these uncertainties follows.

CHAPTER 2. EXPERIMENT DESCRIPTION

The MSRE [1], shown in Figure 1, was primarily constructed of Hastelloy N (also called INOR-8), a nickel-based alloy. Salt entered the reactor through the fuel inlet at the top of the reactor, flowed down an annulus to the bottom head, flowed up through fuel channels formed by graphite blocks, and continued through the top head to the fuel outlet.

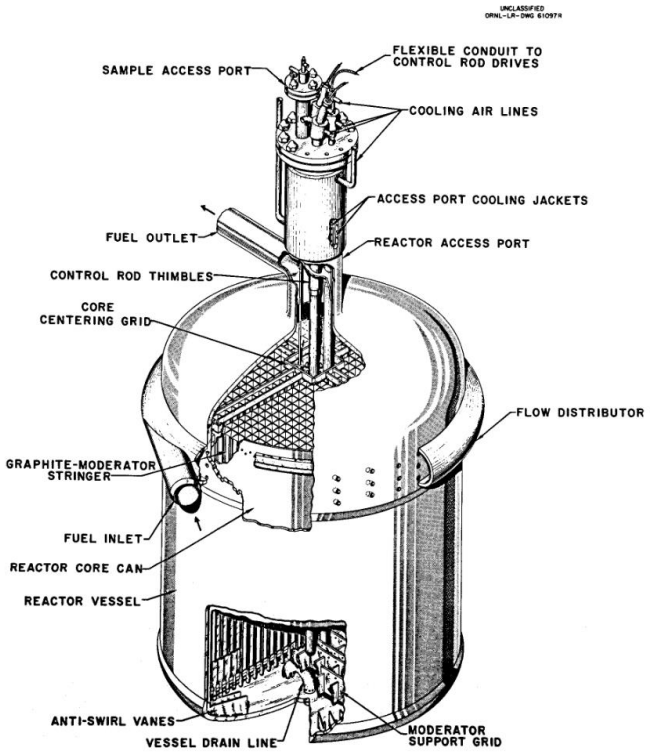

Figure 1: MSRE Reactor Vessel (Figure from [1])

The ^{233}U zero-power physics experiments were conducted in late 1968, beginning with the zero-power critical experiment [2]. The reactor was slowly brought to critical via the addition of uranium stock in the reactor pump bowl.

For this work, a model of the critical experiment was made in MCNP 6.1, using the ENDF/B VII.1 cross section library [3], [4]. A description of the reactor geometry is given in Section 2.1. The experimental data from the ^{233}U critical experiment are presented in Section 2.2.

2.1 Geometry Data

The geometric data for the reactor was compiled largely from [1]. Two caveats must be given in the use of this document. First, it was released before the experiment took place, and thus in some cases may not (and in fact does not) correspond to an "as-operated" description. Second, even if it did correspond to an "as-operated" description, on its own this document is not sufficient to accurately reconstruct a full description of the reactor. As such, these gaps must be filled in from other documentation, or reasonable assumptions must be made.

All dimensions presented in this section are cold dimensions. Geometric and material elements of the reactor were modeled exactly when fully specified in the documentation. In some cases where there exists missing information, assumptions are made and noted. If the effect of the assumption on the resulting experimental uncertainty was felt to be likely non-negligible, an analysis of the uncertainty was performed. A list of the assumptions that were felt to have a negligible reactivity effect can be found in Appendix A. The MCNP model accounts for the differential thermal expansion resulting from the varying coefficients of thermal expansion.

2.1.1 Reactor Vessel

From [1], the MSRE reactor vessel has an inner diameter of 58". Shown in Figure 2, the vessel includes an ASME tori-spherical top and bottom head. The top 16" of the cylindrical wall is 1" thick, while the remaining height is $^{9}/_{16}$" thick. Specific values for the height of the vessel and the design specifications of the two heads are areas of ambiguity and are discussed in Section 3.1.1.

At the top of the reactor vessel, there is a half-toroidal flow distributor of inner radius "about 4 in." [1]. Additional documentation states that the cross sectional area of the volute (assumed to be thermally expanded) is 26.0" inches, which implies an inner radius of 4 $^{1}/_{32}$" [5]. The precise vertical location of the distributor is ambiguous and was assumed to be in the middle of the 16" height of extra thickness vessel wall.

2.1.2 Lower Head

In the lower head of the reactor vessel, there are 48 evenly spaced (radially) anti-swirl vanes [1]. These vanes are fabricated from $^{1}/_{8}$" thick INOR and extend radially 11" inward from the reactor vessel inner wall. The upper contour of the vanes is never described, and can only be inferred from diagrams, such as Figure 3. For this model, the upper contour is assumed to be a cone, which intersects the inner edge of the vanes at the same height as the bottom of the core support grid and intersects the outer edge of the vanes at the same height as the beginning of the lower head.

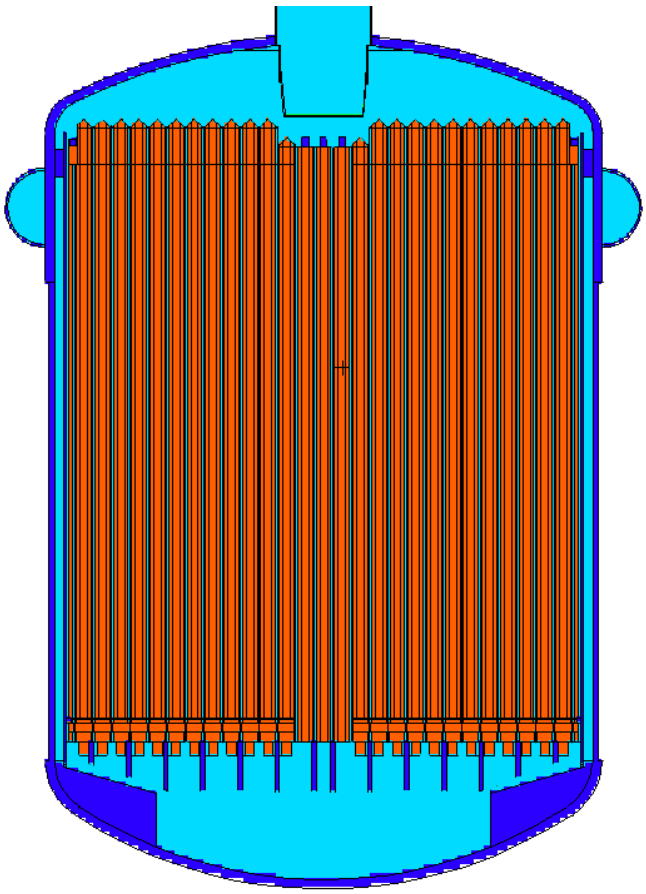

Figure 2: MSRE Reactor Vessel

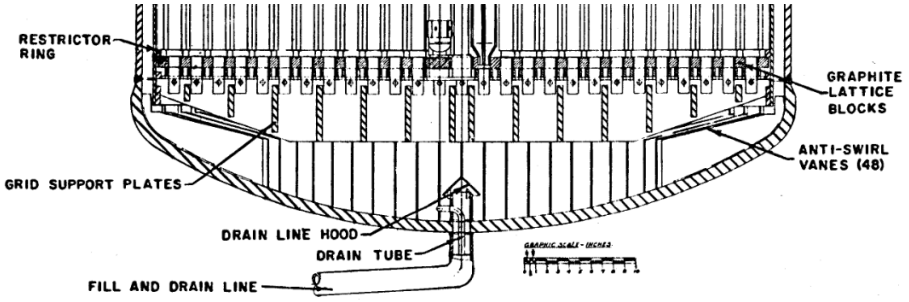

Figure 3: Vessel Lower Head (Figure from [1])

The lower head contains two major components: the 48 anti-swirl vanes, and the core support grid. These elements can be seen in Figure 2 and Figure 3, and Figure 4. The anti-

swirl vanes are fabricated from $^{1}/_{8}$" thick INOR and extend radially inwards 11" towards the core center [1]. An upper slope was assumed based approximately on the slope seen in Figure 3.

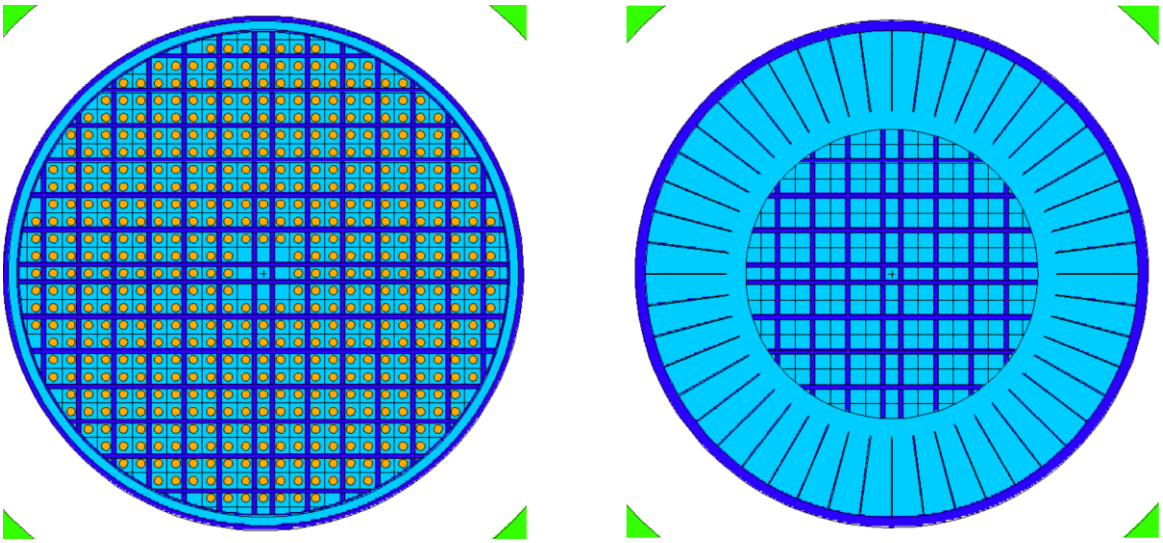

Figure 4: Lower Head - (Left) Just Below Horizontal Graphite (Right) Elevation of Vanes

The core support grid is fabricated from $^{1}/_{2}$" thick INOR plate. Based on Figure 3, it was assumed that the plates begin 1" from the core centerline and repeat every 2" after that. They are 5 $^{9}/_{16}$" thick at the center of the core, and 1 $^{5}/_{8}$" thick at the periphery. The model plates were truncated by a cone to match the slope seen in Figure 3. These assumptions are assumed to be reasonable and are discussed in Appendix A. The support grid poses particular difficulty for modeling, especially when handling differential thermal expansion. This is because the repetition associated with the INOR grid and repetition associated with the doweled extension into the support grid region have different coefficients of thermal expansion, and thus cannot be concisely handled with typical repeated geometry features, instead requiring verbose description plate-by-plate as was modeled in this analysis.

2.1.3 Core Can

The core can (Figure 2) is also fabricated from INOR. It has an inner diameter of 55 $^{1}/_{2}$", an outer diameter of 56", and a height of 67 $^{15}/_{16}$" [1]. For this model, it was assumed that the top of the core can was coplanar with the bottom of the upper head of the reactor vessel. Affixed to the bottom of this can is the core support grid, discussed above. The core can is affixed to the reactor vessel at the top by 36 support lugs, represented in this model as chunks of INOR that fill the space between the vessel and can.

2.1.4 Core Graphite

The graphite core is primarily made up of 2" x 2" cross sectional graphite stringers (Figure 5), with fuel half-channels machined on each lengthwise face [1]. The tops of the bars are tapered in a pyramid shape, to prevent salt from standing on them in the case of a core drain. The stringers include a 1" diameter doweled section at the bottom, which nest into holes in two horizontal layers of graphite bars, upon which the stringers rest when not immersed in salt.

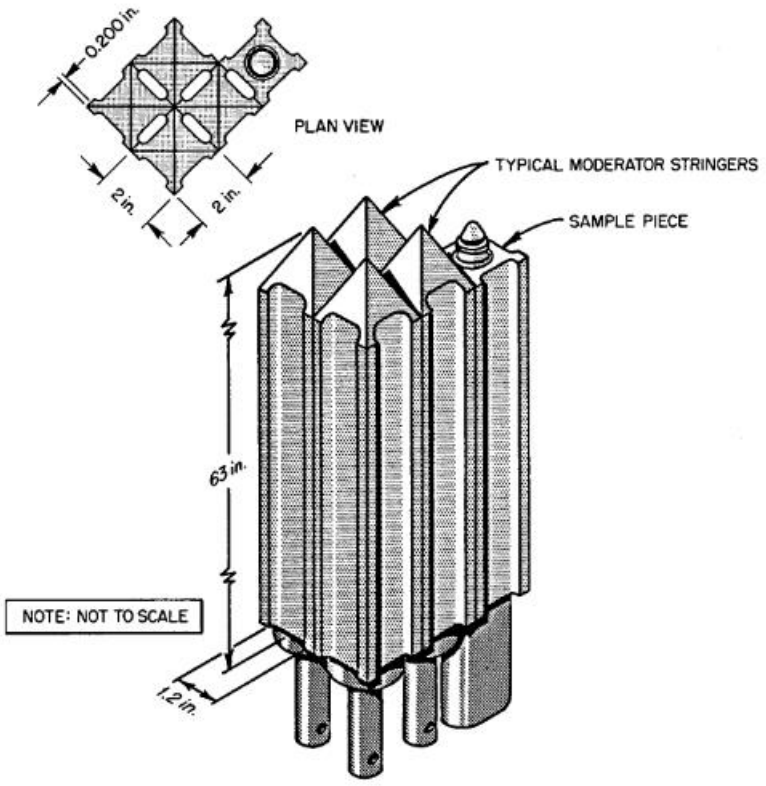

Figure 5: Graphite Stringer Arrangement (Figure from [1])

A typical graphite stringer has 3.5" (assumed) of doweled section, a $^{3}/_{8}$" (assumed) cylindrical section which rests above the horizontal graphite, 62 $^{1}/_{8}$" (from [6]), and a 1" (assumed) tapered pyramidal top section, for a total length of 67". The assumed figures were made to best match various figures (including Figure 3) while adhering to the overall length of "about 67 in." from [1].

The regular pattern of stringers is interrupted in the center of the core, where 5 special stringers are used instead. These stringers are 64 $^{1}/_{2}$" long, do not have the doweled nor cylindrical sections at the bottom (resting directly on the INOR support grid), and are drilled and tapped with a $^{3}/_{4}$" INOR lifting stud. The stringers surrounding the 4 slots in the core center for the 3 control rod thimbles and sample basket also have one face

machined with a part-cylindrical cutout, instead of a regular fuel half-channel, seen in Figure 6. This is to provide a full cylindrical opening for the thimble or basket.

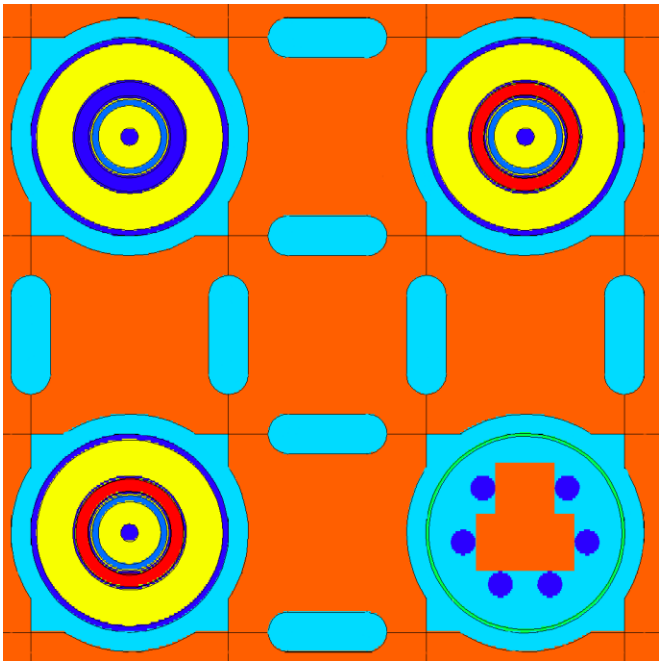

Figure 6: Fuel Channels in Center of Core

Additionally, stringers along the 2 diameters of the reactor are taller than standard stringers. Upon being buoyed by the salt, they nest into a graphite centering bridge, about which there is no provided information. It was assumed that these stringers are 2” taller than standard stringers.

Most of the graphite stringers rest on 2 layers of horizontal graphite bars at right angles to each other, with a 1” x 1 $^{5}/_{8}$” cross section. The top layer can be seen in Figure 7. These graphite bars are drilled with 1” diameter holes, which accept the 1” diameter doweled section of the graphite stringers. The bars rest directly on the core support grid. Additionally, [5] states that the top layer of graphite is drilled with 0.104” diameter holes

directly beneath the N-S fuel channels, to equilibrate flow imbalance between these N-S channels and E-W channels.

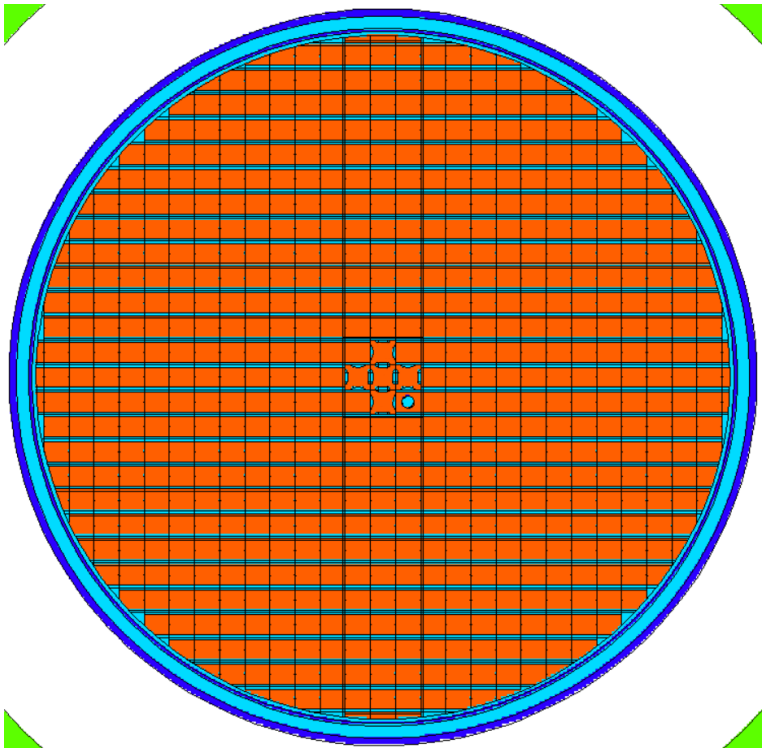

Figure 7: Horizontal Graphite

2.1.5 Control Rods

Information about the control rods comes largely from [1], but is supplemented by a document detailing the manufacture of the control elements [7]. The control rods (Figure 6 and Figure 8) consist of control elements threaded bead-like on a stainless-steel hose, with a braided Inconel cable in the center.

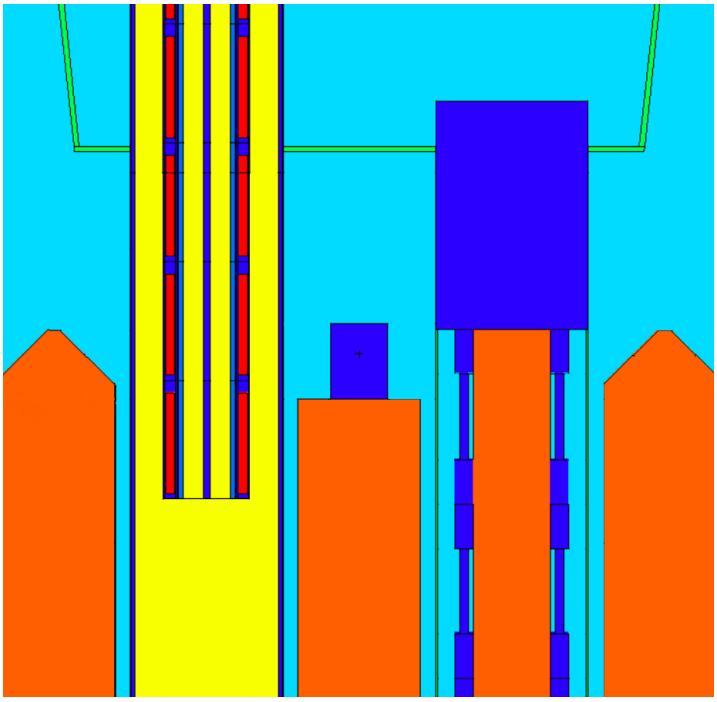

Figure 8: Control Rod and Sample Basket

The poison bushings themselves are 70% Gd_2O_3, 30% Al_2O_3. Each control element contains a stack of 3 bushings, measuring 0.84” inner diameter, 1.080” outer diameter, and 1.325” tall. The bushing stack is encased in an Inconel shell, which brings the total height of each element to 1.562” [7]. The precise location of the control rods during the experiment is discussed in Section 3.1.2.

Each control rod is contained in the core within a control rod thimble, 2” in diameter and filled with cell gas. These thimbles extend through the outlet nozzle, upper head, and into the core.

2.1.6 Sample Basket/Irradiation Specimens

The sample basket is the most notable model element in which [1] does not represent an “as-operated” description of the reactor. [8] describes the samples that were in the

reactor at the time of experiment, and [9] describes how the basket was re-designed (after the release of [1]) after the assembly had to be replaced. This assembly is described in Section 3.1.3.

2.1.7 Upper Head/Outlet Nozzle

The shape of the upper head is discussed in Section 3.1.1. It contains a perforated INOR strainer basket and strainer disk (Figure 2 and Figure 9), which is described (albeit not completely) in [1].

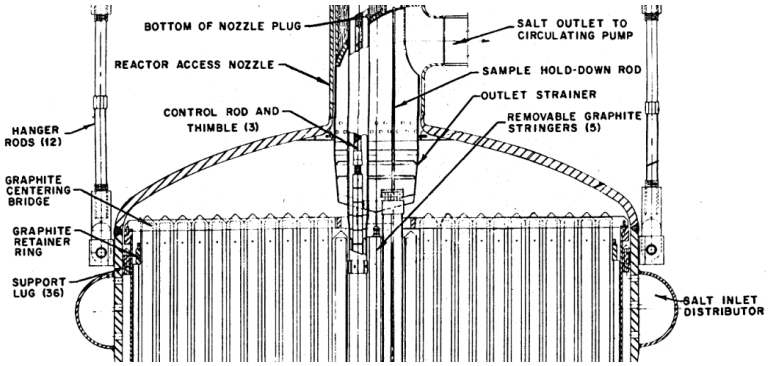

Figure 9: Reactor Vessel Upper Head (Figure from [1])

The strainer disk is 18” in diameter and has a 9.52” diameter cutaway to accept the strainer basket. The strainer basket is 9.52” in diameter at the top, 8.5” in diameter at the bottom, and about 7” deep [1]. The reference also describes a cross shaped extension below the strainer basket to keep the 5 removable center graphite stringers in place, although not in enough detail to create a defensible model recreation. The basket has 4 cutouts at the bottom to allow the 3 control rod thimbles and sample basket to pass through it.

The outlet nozzle is 10” in diameter, with a 5” diameter side outlet. Above the side outlet is the outlet nozzle plug, which is described as “hollow and filled with insulation”.

This insulation was assumed to be the same insulating material as coats the thermal shield, discussed immediately below.

2.1.8 Reactor Surroundings

The reactor is surrounded by a thermal shield, “about 10.4 ft. outer diameter, 7.5 ft. inner diameter, and 12.5 ft. high overall.” [1], seen in Figure 10. The shield is constructed of 1” thick stainless-steel plate, with a 14” annular space filled with carbon steel balls cooled by water. The inside of the shield is lined with 6” of expanded silica insulation, branded “Careytemp 1600 °F”.

In between inner surface of the insulation and the outside of the reactor vessel, there are electrical resistance-type heaters [1]. Although the specifications of the heaters are described, their specific configuration is not described in enough detail for them to be recreated in the model.

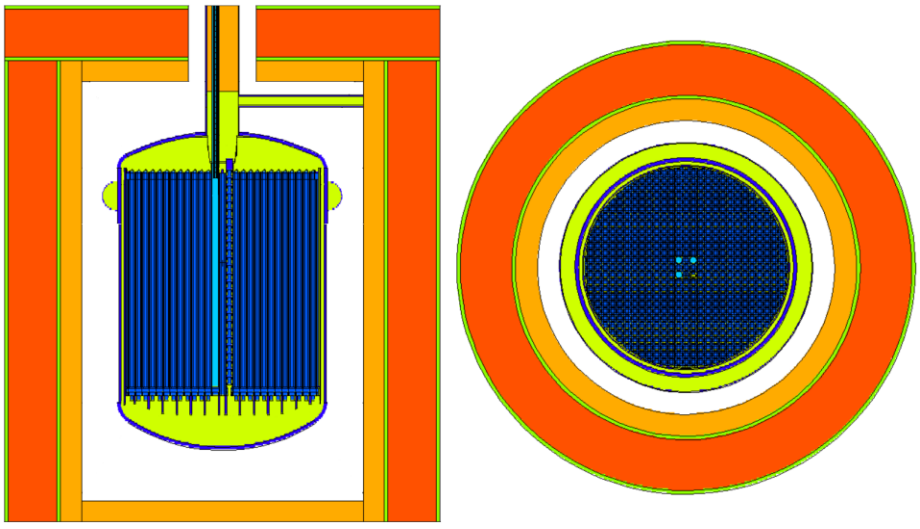

Figure 10: Thermal Shield and Insulation

2.2 Critical Experiment Data

Initial criticality with ^{233}U was obtained on October 2, 1968 [2]. The bulk of the uranium stock required for criticality (about 33 kg of feed material) was added via the drain tank equipment. The remaining uranium needed for criticality was added via four 95 g capsules, for a total reported uranium loading of 33.26 kg ± 0.015 kg. The reported volume of the fuel salt inventory was 77.6 ± 0.5 ft^3. The core temperature (assumed in documentation to be isothermal) was 1202 °F ± 2 °F. One control rod was inserted "a distance equivalent to about 0.015 of its total worth", which was reported to be an effect worth 0.04% ± 0.02% $\delta k/k$. A small, unknown void fraction was also associated with the fuel salt at the time of experiment. The documentation estimates this to be 0.1% ± 0.1% volume.

Additional information about the critical experiment can also be obtained from parts of [10]. This document provides general chemistry information about the entire experiment lifetime. These two documents are used to stitch together best-estimate values for many elements discussed below. Where these two documents combined are still insufficient to reconstruct a full description, other related documentation has been used to fill in gaps.

CHAPTER 3. NOTABLE GAPS AND EXPERIMENTAL UNCERTAINTIES

In constructing a model of the experiment, several geometric and material input elements stick out as notable, either because they represent a documentation gap that requires assumption, they represent a large source of experimental uncertainty in the resulting calculation, or the reconstruction of the best-estimate values for the data point is not direct. These elements are discussed in detail below.

For this analysis, many of the material uncertainties presented in the experimental documentation are assumed to be bounding values. Thus, per [11], the standard uncertainty associated with a value bounded by $a < x < b$ in this analysis is expressed as:

$$\Delta x = \frac{b - a}{2\sqrt{3}}$$

Where an experimental value is expressed in documentation as $x \pm \Delta x$, this is interpreted as a representation of the bounding values of the data point, so the uncertainty used in calculating the standard uncertainty in k_{eff} is again scaled by a factor of $\sqrt{3}$.

However, a number of the experimental uncertainties presented below are not due to uncertainties in reported values but instead are due to gaps in documentation. In these cases, per [11], the experimental uncertainty is handled with judgement as to the confidence of the best-estimate value.

3.1 Geometric Data

3.1.1 Reactor Vessel Height and Head Size

In [1], the reactor is described as "about 94 in. high," and having two "torospherical ASME flanged and dished heads." Flanged and dished heads can be fully described by their thickness t, outside head radius r_{outer}, inside crown radius r_{crown}, and inside knuckle radius $r_{knuckle}$. These can be combined in the following Pythagorean relationship:

$$((r_{crown} + t) - h)^2 + (r_{outer} - (r_{knuckle} + t))^2 = (r_{crown} - r_{outer})^2 \qquad (1)$$

The constants t = 1" and r_{outer} = 30" are given in [1]. The values for r_{crown} and $r_{knuckle}$ depend on the specific style of head used. If what is traditionally called a "Standard ASME Flanged and Dished Head" are used, then these values are $r_{crown} = 2\, r_{outer}$, and $r_{knuckle} = 0.03\, r_{outer}$. The above relation can then be solved for $h = 10.643"$. This poses a problem for the verbal description from [1] of "about 94 in. high" when combined with Figure 5.4 from that document (shown in part in this document as Figure 3 and Figure 9). If this style of head was used on both top and bottom, that would leave about 72.7" of the cylindrical straight-walled sections. The figure indicates that this section only about covers the 68" length of the core can, giving a discrepancy of about 4.7".

In order to rectify this discrepancy, various combinations of vessel heights and head styles were attempted, two of which can be seen in Figure 11. Some of these permutations were associated with reactivity differences of up to 80 pcm (Δk). For the nominal model, the description that fit most descriptions was determined to be a standard head on top (required to allow the strainer basket to intersect the sample basket, as pictured and described), a Korboggen head ($r_{crown} = 1.6\, r_{outer}$, and $r_{knuckle} = 0.308\, r_{outer}$.) on bottom, and a fixed vessel height of 92".

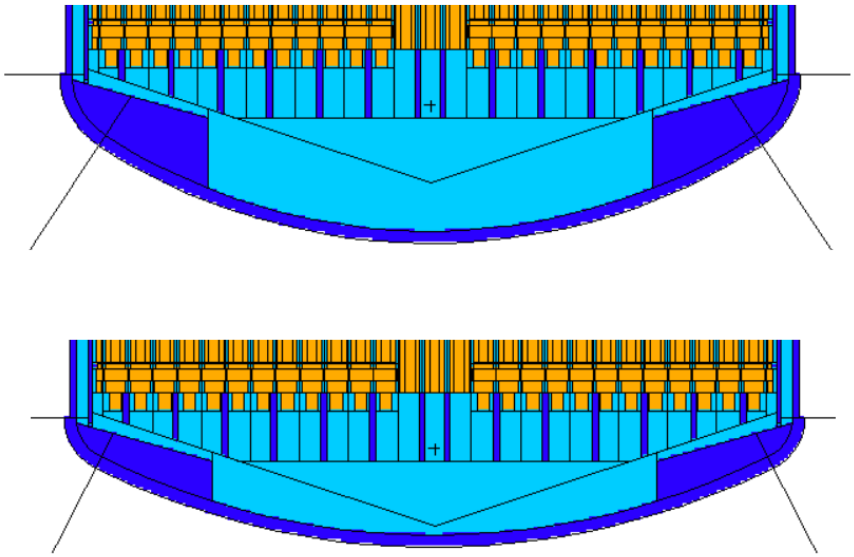

Figure 11: Bottom Heads - (Top) Korboggen (Bottom) ASME Standard

Table 1 presents the assessed uncertainty associated with the reactor vessel dimensions, with the uncertainty assessed as the spread among the various combinations that all fit the documentation.

Table 1: Reactor Vessel Uncertainty

Model Item	**Input Value**	**Standard Uncertainty, Δk_{eff}**
Combined Vessel Shape/Size	92” height, ASME Top Head, Korboggen Bottom Head	$\pm$ 80 ($\pm$ 9) pcm

3.1.2 Control Rods

In the description of the critical experiment, a precise description of which control rod was inserted and to what degree is not provided. Instead, it is only stated that one control rod was inserted to about 0.015 of its total worth. This description can be cross

referenced by physical measurement of the control rod calibration data (Figure 12), to determine that this corresponds to about 3.7” inserted.

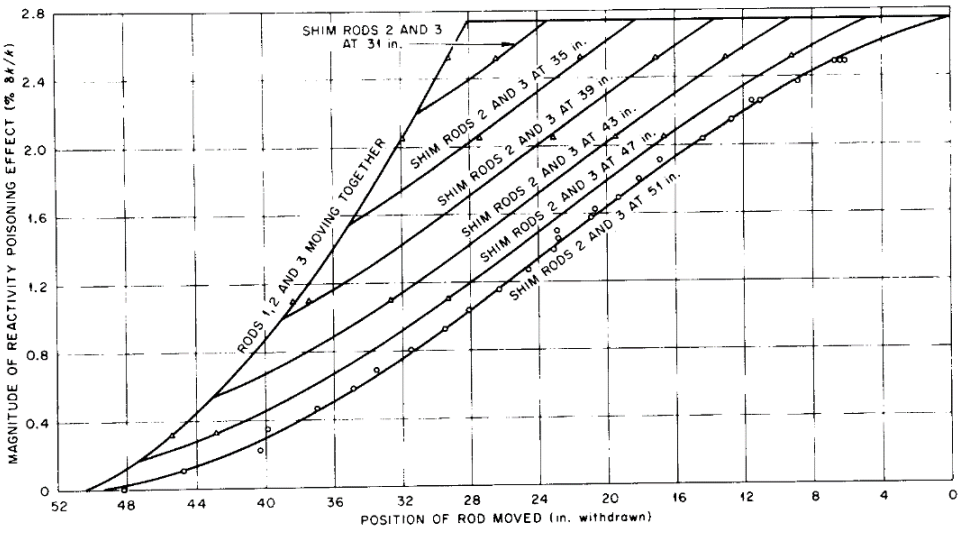

Figure 12: Control Rod Worth (Figure from [2])

However, one rod inserted to this depth was calculated (via comparison against an all-rods-out calculation) to have a reactivity effect of 106 ± 9 pcm. This discrepancy is non-negligible from the predicted value due to control rod calibration data (and confirmed elsewhere in the literature) of 40 ± 20 pcm.

To further explore this, a brief analysis of the calculated control rod worth was performed to generate a new worth/distance chart, seen in Figure 13. From this chart, it is observed that the experimentally reported control rod worth (40 ± 20 pcm) is obtained between 1” and 2.5”.

Ordinarily, a calculated control rod worth differing from an experimentally observed one would not necessarily introduce a source of model uncertainty for a criticality benchmark, as long as the geometry surrounding the control rod insertion was well

documented. However, the fact that we are relying on this data to reconstruct a position for the control rod means that this is relevant to the uncertainty analysis, as the process by which the experimenters equated the critical experiment control rod worth to an insertion distance is not well documented. Since we thus must rely on these measurements, uncertainty is introduced.

For the sake of literature self-consistency, the 3.7" distance is selected as the best-estimate value for the nominal model. The most conservative reasonable estimate of uncertainty is the largest difference between the calculated control rod worth and the predicted control rod worth.

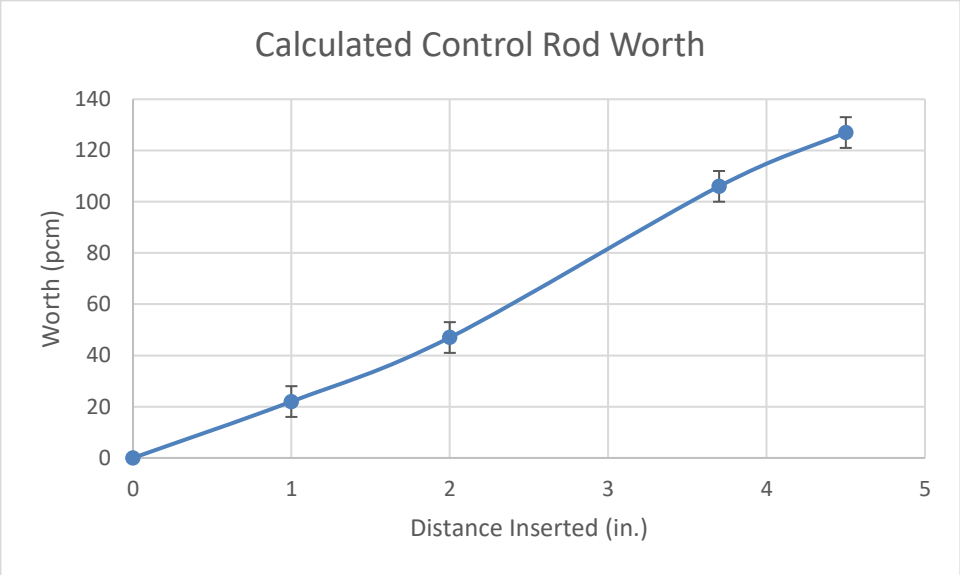

Figure 13: Calculated Control Rod Worth

Table 2 presents the assessed uncertainty associated with the location of the control rod. As discussed above, this value is set to the largest difference between the calculated and predicted control rod worths, $106 - (40 - 20) = 86$ pcm.

Table 2: Control Rod Poisoning

Model Item	Input Value	Standard Uncertainty, Δk_{eff}
Control Rod Poisoning	Distance corresponding to 40 ± 20 pcm (3.7")	± 86 (± 9) pcm

3.1.3 Sample Basket/Irradiation Specimens

As mentioned above, the sample basket is one area in which [1] does not correspond to an "as-operated" description. The samples that were in the reactor are described in [8], but this description is not sufficient to recreate the contents in detail. Further information can be gleaned from [9], including Figure 14. The sample basket is 2" in diameter, 0.065" thick. The model sample basket and contents can be seen in Figure 6 and Figure 8.

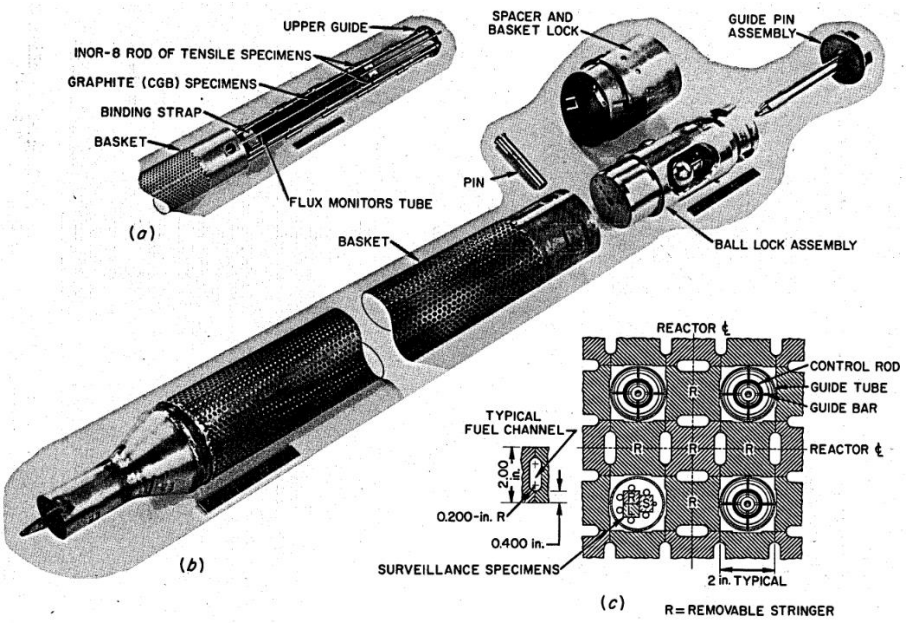

Figure 14: Sample Basket and Specimens (Figure from [9])

Now, [8] and [9] describe the samples as 62" long. The INOR samples are $^1/_4$" diameter, with periodic reduced sections 1 $^1/_8$" long x $^1/_8$" in diameter. It is assumed based

on the numbering scheme that there are 27 of these reduced sections, and that these reduced sections are symmetrically distributed in 27 evenly split sections of each rod.

Apart from being 62” long, no other dimensions are provided for the central graphite test specimens, other than that they are “made up of various pieces that are joined by pinning and tongue-and-groove joints.” In the model, they are represented as straight bars with assumed dimensions 62” x 0.5” x 0.6”, based on physical measurement of the diagram in Figure 14, as well as a similar diagram in [12]. Since they span the highest-flux region of the core, changes to these dimensions are relatively impactful. If instead the dimensions 62” x 0.4” x 0.6” are used, representing only a change of 0.1” in one dimension (as in Figure 15), there is a change in reactivity of 37 ± 9 pcm.

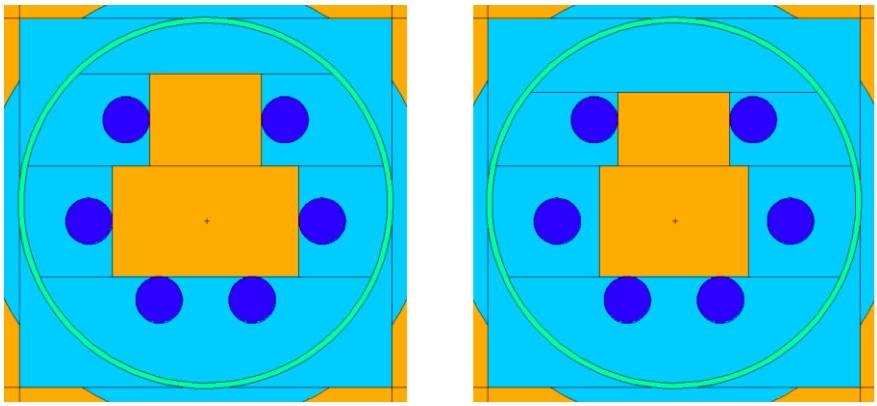

Figure 15: Test Specimens - (Left) Nominal, Assumed (Right) Reduced

It is observed from Figure 14 that the specimen bundle also includes other elements such as binding straps and flux monitor tubes. These elements are not described in enough detail to model but are likely to have a large impact on reactivity relative to their size, for the same reasons discussed above. It is reasonable to think that these additions (particularly the flux monitor tubes) may contribute another 50 pcm of uncertainty.

Table 3 presents the assessed uncertainty associated with the sample basket and its contents. This value is assessed as the calculated reactivity change due to the sample perturbation of 37 ± 9 pcm, plus an additional estimated 50 pcm due to the other unmodeled contents of the sample basket.

Table 3: Sample Basket and Contents

Model Item	Input Value	Standard Uncertainty, Δk_{eff}
Sample Basket and Contents	INOR Rods, Graphite Samples 62” x 0.5” x 0.6”	$\pm$ 87 ($\pm$ 9) pcm

3.2 Material Data

3.2.1 Salt Nominal Composition

The exact composition of the salt at the time of criticality is not as well documented as the initial ^{235}U pre-power experiments at the beginning of the experiment. As such, it is necessary to reconstruct a salt description from scratch, using primarily information from [10], modified to fit the chronology described in [2]. The guiding logic behind the reconstruction is that the primary change in molar composition of the salt during the ^{233}U operation phase was the change due to burning fuel. As such, a good estimate for the salt composition at the time of criticality can be obtained by starting with the average composition of the salt during ^{233}U power operations, and removing the correct proportion of fuel stock in order to obtain the correct uranium concentration reported to be in the reactor by [2].

First, we start with the uranium in the fuel salt. Table 1 from [2] provides the isotopic composition of the feed material for the experiment.

Table 4: Uranium Feed Composition (Table from [2])

Isotope	Weight Percent
232	0.022%
233	91.49%
234	7.6%
235	0.7%
236	0.05%
238	0.14%

Now, [2] also describes two other sources of U. The first is 1.935 kg of uranium heel leftover from ^{235}U operations that remained in the reactor system during the cleaning and was thus not removed. This uranium was briefly reported in [2] to have an isotopic assay of 32.97% ^{235}U, 66.23% ^{238}U. For this work, the assay used was the assay reported in Table 7.5 of [10] to be the uranium assay at the end of ^{235}U operations: 0.343% ^{234}U, 32.705% ^{235}U, 0.483% ^{236}U, 66.469% ^{238}U. This assay was used over the previous assay from [2] in order to accurately fill in values for ^{234}U and ^{236}U.

The second additional source of uranium during the experiment was an addition of 0.89 kg of depleted uranium, added to obtain the correct isotopic abundances necessary for a set of other experiments. The specific assay was not reported, so a typical depleted uranium assay of 0.3% ^{235}U, 99.7% ^{238}U [13] was used.

With this, we can construct a complete picture of the uranium in the reactor at the time of the critical experiment:

Table 5: Uranium Isotopic Composition Reconstruction

Uranium Source	Amount (kg)	^{232}U	^{233}U	^{234}U	^{235}U	^{236}U	^{238}U
Residue [10]	1.935			0.343%	32.705%	0.483%	66.469%
Depleted	0.890				0.3%		99.7%
Stock	33.260	0.02%	91.49%	7.6%	0.7%	0.05%	0.14%
Total	36.085	0.02%	84.33%	7.02%	2.41%	0.07%	6.15%

Now, this analysis assumes the reported 33.26 kg of added uranium refers ONLY to the added stock and does not include either the residue from ^{235}U operations or the additional depleted uranium. It is desirable to bolster this assumption with additional data. Table 3.1 of [10] can aid in this endeavor.

Date	Sample	Equiv. Full Power Hr	(Weight %) Li	Be	Zr	U Nom.	U Obs.	F	Σ	(ppm) Fe	Cr	Ni	Pu	ΣU in Circulation	ΔU (kg)
9/19/68	FP 15-10		10.45	6.44	11.28	0.768	0.764	67.18	96.13	125	29	60	102	32.862	+4.489
9/20/68	FP 15-11		Capsule No. 30 Enrichment No. 1												
10/1/68	FP 15-12		-	6.18	11.07	0.770	0.764	66.68	-	109	31	70	120	32.952	+0.090
10/2/68	FP 15-13		Capsule No. 28 Enrichment No. 2												
10/2/68	FP 15-14		Capsule No. 25 enrichment No. 3												
10/2/68	FP 15-15		Capsule No. 26 Enrichment No. 4												
10/3/68	FP 15-16		Capsule No. 24 Enrichment No. 5												
10/3/68	FP 15-17		Capsule No. 23 Enrichment No. 6												
10/5/68	FP 15-18		10.63	6.62	10.94	0.780	0.822	67.61	99.66	159	36	82	106	33.430	+0.478

Figure 16: Composition of the MSRE Fuel Salt (Table 3.1 from [10])

In this chart, the critical experiment occurs with salt composition represented by FP 15-15, after the addition of Capsule No. 26. The "ΣU in Circulation" column appears to indicate that 33.26 kg refers to all uranium in the system. However, this is disputed by the nominal uranium weight percent represented in the table. If this nominal weight percent (interpolated to be 0.7765% at the time of the experiment) were to be believed, the reported 15.15 g U /L of [2] (corresponding to 33.26 kg) would indicate a total salt density of 1.94 g/cm^3. Although the specific density of fuel salt with an appropriate uranium concentration for ^{233}U operations is not reported, this value is unreasonably low. Other auxiliary

calculations in [10] (including concentrations of plutonium, etc.) put this value at between 2.10 g/cm^3 and 2.15 g/cm^3. If we instead assume that the 15.15 g/L and 33.26 kg values refer only to the amount of enriched ^{233}U stock added, the total U mass of 36.085 kg combines with the reported volume of 77.6 ft^3 and weight percent of 0.7765% to yield a density of 2.112 g/cm^3. This value is much more reasonable, and thus lends credibility to the idea that the masses and concentrations reported in [2] do not include the residue nor added depleted uranium. Additionally, the value reported in this "ΣU in Circulation" column for the beginning of ^{233}U power operations also differs from corresponding values reported elsewhere for the purposes of uranium accounting, lending credence to the idea that this is not representative of all uranium in the reactor. With this, we continue with the assumption that the uranium residue and depleted uranium addition are not included in these figures. (Note, if the other line of thinking is followed, this represents a calculated reactivity delta of about -2500 pcm.)

Constructing a best-estimate nominal composition for the rest of the fuel salt poses a problem, as information about the salt composition at this period (that is, during the ^{233}U loading phase, but before full-power operation) is relatively scarce. For example, it is observed that the master table of salt composition analyses (Figure 16 in this document) doesn't have any numerical data on the date of criticality. As such, for this analysis, it was determined that the best reconstruction method would be to begin with the average salt composition during ^{233}U full-power operations and work backwards to the date of criticality by removing known additions.

We begin with the average composition of the fuel salt for ^{233}U power operations from Table 3.2 of [10]. We then reduce the values of UF_4 and LiF in proportion according

to the 27% UF_4 - 73% LiF (mol%) values reported in [14] as the composition of the enriching salt, such that the weight percent of uranium is reduced from the full-power operation value of 0.809% to the critical experiment value of 0.7765%, shown in Table 6.

Table 6: Reduction of Salt Constituents to Critical Experiment Conditions (mol %)

	LiF	**BeF_2**	**ZrF_4**	**UF_4**	**Σ**
Run 16-18	65.08% ± 0.91%	29.93% ± 0.93%	4.85% ± 0.14%	0.137% ± 0.004%	99.997%
Reduced	65.065%	29.93%	4.85%	0.131%	99.976%

Converting this reduced composition to weight percent yields the best estimate for the fuel salt used in this analysis (subject to the specific isotopic modifications discussed later in Section 3.2.3).

The largest uncertainty involved with this reconstruction is the uncertainty associated with the volume of the fuel salt at the time of experiment, 77.6 ft^3 ± 0.5 ft^3. Now, although the quantity of uranium in the loop is relatively well known, the amount of carrier salt in the loop is less well known. As such, these uncertainties are examined independently.

The amount of uranium in the loop at the time of the experiment, per above, is 36.085 kg. The uncertainties associated with this quantity (0.015 kg for the stock additions, plus whatever uncertainty is reasonably assigned for the other uranium sources) have a negligible effect on the uranium density relative to the uncertainty on the fuel volume. So, the resulting uranium density uncertainty is dominated by the volume uncertainty. These quantities combine for a total uranium density of 16.40 g/L ± 0.10 g/L.

The resulting density probability density can be treated as uniform, since the reported uncertainty on the volume is much less than the volume itself. As such, the uncertainty is

scaled by a factor of $\sqrt{3}$. So, the standard uncertainty is assessed by varying the input value by a value of $(0.10\ {}^{g}/_{L})/\sqrt{3} = 0.06\ {}^{g}/_{L}$.

Keeping the density of the carrier salt constant and only varying the uranium density by 0.06 g/L, this uncertainty is associated with a reactivity effect of 154 ± 7 pcm, as shown in Table 7.

Table 7: Uranium Density

Model Item	Input Value	Standard Uncertainty, Δk_{eff}
Uranium Density	16.40 g/L ± 0.10 g/L bounded	+169 ($\pm$ 8) pcm -126 ($\pm$ 8) pcm

An additional uncertainty arises from the carrier salt density (here, carrier salt is used to refer to all fuel salt constituents besides uranium) at the time of experiment. As stated above, this value is not reported in documentation, and as such must be otherwise determined. Using the interpolated weight percent for uranium of 0.7765%, this results in a total fuel salt mass of 4,647 kg, or a carrier salt weight of 4,611 kg. Table 3.7 of [10] provides a material balance for the MSRE fuel salt that, although it does not provide a specific entry for this time period, corroborates this general range of about 4,650 kg. Elsewhere in [10], different values are provided for this quantity indicates that the uncertainty on this value may be as large as 40 kg. Combining this with the uncertainty in volume, this results in a density between 2.08 g/cm^3 and 2.15 g/cm^3, with a nominal value of 2.112 g/cm^3.

It is assumed that the reported experimental uncertainties represent bounding values, with a uniformly probable distribution between them. The quotient of these probability

distributions is not easily described. As such, it was evaluated numerically. The probability distribution for the carrier salt density (obtained by assuming a uniform distribution of both the volume and salt mass inputs) is seen in Figure 17.

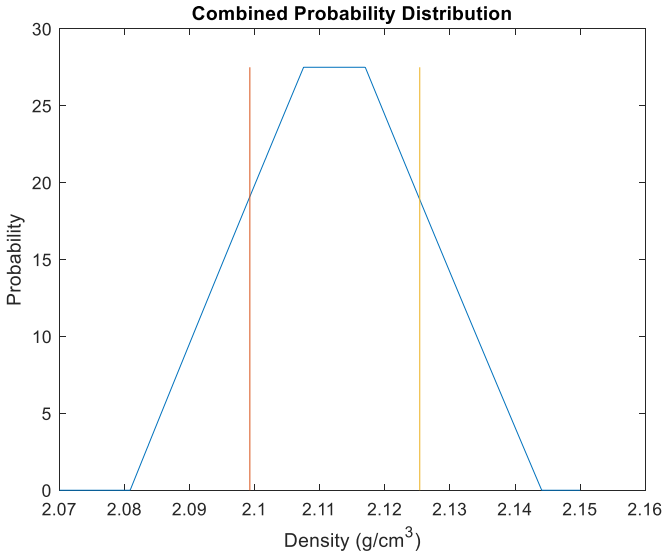

Figure 17: Carrier Salt Density Probability Distribution

The standard uncertainty in k_{eff} associated with this experimental uncertainty was assessed by varying the salt density by a value corresponding to the numerically determined standard deviation of the above distribution of 0.013 g/cm^3.

Keeping the uranium density constant and varying the salt density by 0.013 g/cm^3, this uncertainty is associated with a reactivity effect of 49 ± 6 pcm, as shown in Table 8.

Table 8: Carrier Salt Density

Model Item	Input Value	Standard Uncertainty, Δk_{eff}
Carrier Salt Density	2.112 g/cm^3 ± 0.04 g/cm^3, bounded	+74 ($\pm$ 8) pcm -40 ($\pm$ 8) pcm

Now, since the two densities share an independent variable (the salt volume), these variables are correlated. Per [11], the contribution to the total variance due to covariance is calculated as:

$$\text{covariance contribution} = 2\frac{\Delta k}{\Delta \rho_U}\frac{\Delta k}{\Delta \rho_C}\frac{\partial \rho_U}{\partial V}\frac{\partial \rho_C}{\partial V}u_V^2 \quad , \quad \frac{\partial \rho_i}{\partial V} = \frac{-m_i}{V^2} \tag{2}$$

$$= 2\frac{148\ pcm}{.06\ g/L}\frac{57\ pcm}{13 g/L}\frac{36{,}085\ g\ 4.647E6\ g}{(2200\ L)^4}(14L)^2 = 30{,}300\ pcm^2$$

This quantity is added to the total variance in the calculation of standard uncertainty.

Another major source of uncertainty in the salt reconstruction is due to the uncertainty associated with the initial lithium enrichment in the salt. Due to absorption and tritium transport concerns, the lithium contained in the fuel salt was enriched in ^{7}Li constant, up to a nominal average assay of 99.995% (assumed to be weight percent) [10]. Tables of salt stock in this reference imply a bounding uncertainty value of 0.001%. This standard uncertainty is assessed by varying this enrichment by $0.001\%/\sqrt{3} = 0.0006\%$, as shown in Table 9.

Table 9: Li Enrichment

Model Item	Input Value	Standard Uncertainty, Δk_{eff}
^{6}Li Content	0.005% ± 0.001%, bounded	+312 ($\pm$ 8) pcm -263 ($\pm$ 8) pcm

With the uncertainty information provided in [10] and [14], it is possible to also reconstruct uncertainty information about individual isotopic densities. However, often these are about an order of magnitude less than the uncertainty of the overall densities described above, and as such are not expected to contribute a large an uncertainty to the overall analysis.

3.2.2 Graphite Density

The reactivity effect of the uncertainty in the graphite density is simple to describe, but large in magnitude. Reference [1] describes the bulk density of the MSRE core graphite as 1.83-1.89 g/cm^3. For this analysis, these are treated as bounds on the range, with a midpoint best-estimate value of 1.86 g/cm^3 used. The associated standard uncertainty can then be assessed by varying the graphite density by a value of $0.03\,{}^{g}/_{cm^3}\,/\sqrt{3} = 0.017\,{}^{g}/_{cm^3}$, as in Table 10.

Table 10: Graphite Density

Model Item	Input Value	Standard Uncertainty, Δk_{eff}
Graphite Density	1.86 g/cm^3 ± 0.03 g/cm^3, bounded	+375 (± 8) pcm -397 (± 8) pcm

3.2.3 Isotopic Modifications

In reconstructing the material input data for the model, one must account for the isotopic changes that result from the 72,440 MWhr of previous operation with ^{235}U fuel salt. The original reactivity balance calculations [15] provide calculated estimates for the

volume-averaged thermal flux in the entire fuel salt loop, as well as in only the graphite-moderated region. This flux can be used to estimate burn of key isotopes in the overall reactivity balance. The two most important burnout isotopes are presented below.

3.2.3.1 Graphite Boron Burnout

The graphite used in the MSRE nominally initially contained 0.00008% boron (natural isotopic distribution) by weight [1]. For the graphite composition, this can be reduced (assuming uniform burn of the graphite) as:

$$\frac{N_B}{N_{intial}} = \exp\left(-\left(2.00E12\,\frac{n}{cm^2 \cdot s \cdot MW} \cdot 72{,}440\ MWhr\right)(362.4\ b)\right) = 0.8278 \qquad (3)$$

The nominal effect of this burnout (relative to an unburned model) is 78 ± 9 pcm.

Now, the assumed uniform burn of the graphite ignores the locality of the effect. Since there is more burnout in the high flux region of the core, this kind of global treatment underestimates the reactivity effect associated with this change. To accurately assess this phenomenon, a representation of the core environment during ^{235}U operations would be used to obtain a more accurate flux history needed for a boron depletion calculation. To construct such a history would require an in-depth operational history during prior full-power operation with ^{235}U, which is not practical given the level of documentation and uncertainty of the surrounding experimental data.

However, an estimation on the upper bound on this effect can be obtained by burning the entire graphite using a flux equal to the estimated peak flux value. This analysis assumes a peak-to-average flux ratio of 3.64, derived from a homogenous cylindrical

representation of the reactor [16]. Burning all graphite with this estimated peak flux value results in a reactivity effect of 141 ± 9 pcm.

It must also be stated that, since the volume-averaged flux and thermal cross sections derive from the original calculations (due to the impracticality of repeating them), there must also be some uncertainty associated with the crudeness of the method. This analysis credits a relatively conservative 50% uncertainty in the argument of the exponential, which is associated with a 49 ± 9 pcm uncertainty. With this, a lower uncertainty of -49 ± 9 pcm is assessed. For the upper uncertainty, the two uncertainties (49 ± 9 pcm due to flux and cross section estimation and 63 ± 13 pcm due to underestimation) are added in quadrature to obtain an upper uncertainty of 80 ± 16 pcm. These uncertainties are expressed in Table 11.

Table 11: Graphite Boron Burnout

Model Item	**Input Value**	**Standard Uncertainty, Δk_{eff}**
Graphite Boron Burnout	82.8% Boron Remaining	- 49 ($\pm$ 9) pcm + 80 ($\pm$ 16) pcm

3.2.3.2 Fuel Salt ^{6}Li Burnout

The other primary isotope to consider for the reactivity effect of its burnout is the ^{6}Li present in the fuel salt. Unlike the graphite boron burnout discussed previously, this can be considered a decidedly non-local effect due to the motion and mixing of the salt during operation. As such, the lumped ^{6}Li can be reduced as:

$$\frac{N_{\mathrm{Li-6}}}{N_{intial}} = \exp\left(-\left(0.665E12\,\frac{n}{cm^2 \cdot s \cdot MW} \cdot 72{,}440\ MWhr\right)(457.6\ b)\right) = 0.9237 \qquad (4)$$

Once again assessing a conservative 50% uncertainty on the exponential argument due to the flux estimation and cross section, the reactivity effect of the salt ^{6}Li burnout is 177 ± 72 (± 9) pcm, as in Table 12. As with the graphite isotopic burnout, the uncertainty in this value could be driven down with a model of the reactor system during ^{235}U full power operations.

Table 12: Salt ^{6}Li Burnout

Model Item	Input Value	Standard Uncertainty, Δk_{eff}
Salt ^{6}Li Burnout	92.4% ^{6}Li Remaining	± 72 (± 9) pcm

3.2.4 Plutonium Build-up

The processing of the fuel salt in between ^{235}U and ^{233}U operations was observed to have no effect on the amount of built-up plutonium in the fuel salt [2]. As such, all 589g of plutonium leftover from ^{235}U operations is expected to be in the salt at the time of the initial critical experiment. Combining this with the reported salt volume at the time of criticality and the assumed salt density value, this results in an expected plutonium weight percentage of 127 ppm. This is in decent agreement with the nominal value of 128 reported in [10]. Additionally, [10] provides a plutonium assay of 95% ^{239}Pu, 4% ^{240}Pu.

The calculated reactivity effect associated with the presence of this plutonium was 24 ± 10 pcm. This is observed to be less than the predicted reactivity effect in [2] of 0.095% $^{\delta k}/_{k}$. The effect of the uncertainty in these values, which is small due to the careful

plutonium accounting during the experiment, is sufficiently small to be negligible relative to these other dominant effects. However, the discrepancy between the actual and predicted values for the reactivity worth is notable.

3.2.5 Residual Fission Products

The degree to which low-cross-section fission products from the ^{235}U phase of operation remained in the salt during chemical reprocessing is not well known or described [2]. Original calculations for the experiment limit the magnitude of the effect to less than 0.500% $^{\delta k}/_{k}$. The experimenters' confidence in this assessment is not abundantly clear since, although it is mentioned in the report, it is not taken into account in the best-estimate reactivity calculations.

Now, fission product behavior in the MSRE was detailed several years after reactor shutdown in its own report [12]. This report does indicate some level of activity due to fission products during the time frame of the critical experiment. However, this report focuses primarily on inventory activity, and analyzing the ratio to which the observed measurements agree with predicted inventory values. The data surrounding the critical experiment, even in this report, is scant, limited to a few isotopes selected for their radioactivity concerns, rather than reactivity concerns. Attempting to use this data to assess the reactivity effect is likely to result in an incomplete picture.

Given these facts, it is assessed that it is most representative of the underlying data to leave this effect as a positive model reactivity bias, with magnitude less than 500 pcm. As with the other integral effects above, it is possible that this effect might become better understood with a model of ^{235}U power operations. However, this effect poses a unique

challenge to such an analysis, as, even though the salt cleanup process is described, its effect on these fission products is not.

CHAPTER 4. RESULTS AND INTERPRETATION

The calculated k_{eff} of the final nominal model was 1.00957 ± 0.00006. The experimental uncertainties described in Chapter 3 as calculated by MCNP are summarized in Table 13.

Table 13: Experimental Uncertainty Results

Model Item	Input Value	Standard Uncertainty, Δk_{eff}
Graphite Density	1.86 g/cm^3 ± 0.03 g/cm^3, bounded	+375 (± 8) pcm -397 (± 8) pcm
^{6}Li Content	0.005% ± 0.001%, bounded	+312 (± 8) pcm -263 (± 8) pcm
Uranium Density[1]	16.40 g/L ± 0.10 g/L bounded	+169 (± 8) pcm -126 (± 8) pcm
Sample Basket and Contents	INOR Rods, Graphite Samples 62" x 0.5" x 0.6"	± 87 (± 9) pcm
Control Rod Poisoning	Distance corresponding to 40 ± 20 pcm (3.7")	± 86 (± 9) pcm
Combined Vessel Shape/Size	92" height, ASME Top Head, Korboggen Bottom Head	± 80 (± 9) pcm
Graphite Boron Burnout	82.8% Boron Remaining	+ 80 (± 16) pcm - 49 (± 9) pcm
Salt ^{6}Li Burnout	92.4% ^{6}Li Remaining	± 72 (± 9) pcm
Carrier Salt Density[1]	2.112 g/cm^3 ± 0.013 g/cm^3	+74 (± 8) pcm -40 (± 8) pcm
Total:	-	+579 (± 29) pcm -550 (± 26) pcm

[1] Per Section 3.2.1, 30,300 pcm^2 must be added to the total variance due to the covariance of these two variables.

Additional uncertainties noted in this analysis but not explicitly examined due to their negligible expected contribution to overall uncertainty are listed in Appendix A.

Propagating the above uncertainties leads to a calculated total experimental uncertainty in criticality due to the discussed elements of $^{+579}_{-550}$ pcm with a statistical uncertainty of 26-29 pcm. The unexamined assumptions (Appendix A) conservatively may add up to 50 pcm on top of this value, bringing the estimated experimental uncertainty up to around 600-650 pcm.

The question must then be raised as to the feasibility of the development of a benchmark problem for this experiment. Typically, an uncertainty due to experimental data this large would not be considered "benchmark quality". Additionally, a large amount of this uncertainty is due to directly reported uncertainties in the experimental data, i.e., the density of the graphite moderator ($^{+375}_{-397}$ pcm) and the uranium density in the fuel salt ($^{+169}_{-126}$ pcm).

Additionally, as mentioned in Chapter 3, the experimenters mentioned an additional contributing source of uncertainty in the overall reactivity balance due to residual fission products. This effect is difficult to assess but is likely to have contributed up to 500 pcm of positive reactivity bias to the model used in this analysis.

CHAPTER 5. CONCLUSIONS AND FUTURE WORK

An MCNP 6.1 model of the ^{233}U initial criticality experiment of the MSRE was built, and k_{eff} for the model was calculated to be 1.00957 ± 0.00006. In the construction of a model for the experiment, several geometric and material input elements are notable, in that they either represent an assumption in the input or a large source of uncertainty. The experimental uncertainty associated with only the elements described in this document was calculated to be at least 550-579 pcm, with an expected total value around 600-650 pcm.

Several key elements cause this high uncertainty. The reactivity effect of the reported values for the graphite moderator density, volume of fuel salt present in the loop, and initial lithium enrichment represent particularly high sources of uncertainty. Using the experimental data as-is is not likely to support the development of what would traditionally be considered as an acceptable benchmark problem.

Now, the large experimental uncertainty involved with modeling this experiment may not be particularly surprising when considering that the documentation was not written with this application in mind. The primary objective of the MSRE was to "demonstrate that the desirable features of the molten-salt concept could be embodied in a practical reactor that could be constructed and maintained without undue difficulty and one that could be operated safely and reliably." [1]. As such, experimental procedures were primarily designed to collect necessary operating information, not necessarily to provide a complete description upon which to build a high-fidelity calculational model.

This notion is compounded when considering the use of data from the ^{233}U phase of operation relative to the ^{235}U phase. Building a high-fidelity calculational model in, essentially, the middle of reactor life is a difficult problem on its own due to several reactivity effects that result from power operations. Indeed, this is explicitly acknowledged in the experimental documentation (albeit in the context of improving nuclear data) when [2] states the following:

> *"Because of the nature of the reactor and the uncertainties resulting from the residual fission products and other effects of prior operation, however, the experiments could not be expected to yield more precise values for the nuclear characteristics of ^{233}U."* [2]

This statement is supported by the additional uncertainties discussed in this document that surround the reactivity effects surrounding prior operation.

This discussion is not complete, however, without noting the relative lack of experimental reactor physics data surrounding the use of molten salt. The MSRE presents an extremely unique source of data in this regard, and the lack of validated experimental data surrounding the use of MSR/FHR materials in a reactor physics experiment means that we need to take advantage of all available data. In this context, the reader may find this particular experiment useful despite the larger experimental uncertainty, at least until such time as new experiments may be conducted. The trade-off between the lack of alternate information and high experimental uncertainty must be considered. With this in mind, it is reasonable that a benchmark problem description based on this experiment could

be developed. It would be up to the user to determine the degree to which the claim of "experimental validation" could be made based on the use of such a problem.

It is concluded that, although this uncertainty would generally be considered unacceptable for the purposes of benchmark experimental description development, the lack of experimental data surrounding the use of MSR materials in reactor physics experiments means that readers may still find the experiment useful for benchmarking tools for MSR applications, at least until such time as new experiments become available.

APPENDIX A: UNEXAMINED ASSUMPTIONS AND SOURCES OF UNCERTAINTY

Some of the assumptions made in the creation of the experimental model were not analyzed for their reactivity effect, because it was expected that their associated standard uncertainty would be small (< 100 pcm). These elements, along with a short statement describing the reasoning for this projection, are seen in Table 14 below.

Table 14: Unexamined Assumptions

Core Can Support Lug Shape	• Low flux region of model • Specific shape not important relative to mass
Anti-Swirl Vane Upper Contour	• Low flux region of model • Specific shape not important relative to mass
Core Support Grid Lower Contour, Spacing	• Specific spacing not expected to be much different than assumed value of 2” • Lower contour is in low flux region • Specific shape not important relative to mass
Inlet Distributor Height	• Low flux region of model • Specific height not expected to be much different than assumed value

Table 14 Continued

Graphite Stringer Cylindrical Section Length	• Low flux region of model • Length of region does not significantly affect fuel/moderator ratio
Raised Diameter Graphite Stringer Additional Height	• Only affects a small number of stringers • Low flux region of model • Height difference not expected to be much different than assumed 2”
Perforated INOR Volume Ratio of 50%	• Specific ratio not expected to be much different than assumed 50% • Overall volume of perforated INOR is very small
Shape of Lower End of Sample Basket	• Low flux region of model • Low volume of only basket material (perforated INOR)
Shape of Sample Basket Upper Fixture	• Low flux region of model • Actual shape of fixture difficult to determine, but unimportant relative to mass

Table 14 Continued

INOR Sample Reduced Section Periodicity	• The total length of reduced section is known based on verbal description • It is reasonable to assume there is some level of symmetry in the placement of these regions, so centralizing the reduced pieces in 27 equal sections is a good representation of any minor physical difference
Shape of Outlet Nozzle Plug	• Low flux region of model • Specific shape of transition to insulation not important relative to presence of large volume
Core Furnace Heaters/Reactor Vessel Support Struts	• Overall effect on reactivity would be to reflect leaked neutrons back into core • The reflection due to the thermal shield and insulation is thought to be much stronger than this reflection effect would be

Table 14 Continued

Individual Non-U Salt Composition	• These constituents have a much smaller reactivity effect than the U in the salt. • The Li contributes uncertainty far more due to its isotopic composition rather than its salt fraction • The Be contributes due to its moderating effect, but this is not expected to contribute more than 100 pcm
Void Fraction	• Unknown nature of the void fraction means that it is best represented by a reduction in density, which is already a larger uncertainty than 0.1%
Core Temperature	• The experimental data lists a temperature reactivity coefficient of $-7.75 * 10^{-5}\ \delta k/k$ / °F. The listed uncertainty of 2 degrees is thus expected to be around 15 pcm.
Plutonium Mass Uncertainty	• The effect due to all plutonium in the reactor was already observed to be small, so an uncertainty on this value would be negligible

Table 14 Continued

Graphite Distortion	• Later documentation [6] indicates that there was insignificant distortion of the graphite at the time of experiment

REFERENCES

[1] R. Robertson, "MSRE Design and Operations Report, Part I. Description of Reactor Design," Oak Ridge National Laboratory, Oak Ridge, TN, 1965.

[2] J. Engel and B. Prince, "Zero-Power Experiments with 233U in the MSRE," Oak Ridge National Laboratory, Oak Ridge, TN, 1972.

[3] e. a. T. Goorley, "Initial MCNP6 Release Overview," *Nuclear Technology*, no. 180, pp. 298-315, 2012.

[4] M. Chadwick, "ENDF/B-VII.1: Nuclear Data for Science and Technology: Cross Sections, Covariances, Fission Product Yields, and Decay Data"," *Nucl. Data Sheets*, vol. 112, no. 12, pp. 2887-2996, 2011.

[5] R. J. Kedl, "Fluid Dynamic Studies of the Molten-Salt Reactor Experiment (MSRE)," Oak Ridge National Laboratory, Oak Ridge, TN, 1970.

[6] H. E. McCoy and B. McNabb, "Postirradiation Examination of Materials from the MSRE," Oak Ridge National Laboratory, Oak Ridge, TN, 1972.

[7] G. M. Tolson and A. Taboada, "MSRE Control Elements: Manufacture, Inspection, Drawings, and Specifications," Oak Ridge National Laboratory, Oak Ridge, TN, 1967.

[8] J. H. E. McCoy, "An Evaluation of the Molten-Salt Reactor Experiment Hastelloy N Surveillance Specimens - Fourth Group," Oak Ridge National Laboratory, Oak Ridge, TN, 1971.

[9] J. H. E. McCoy, "An Evaluation of the Molten Salt Reactor Experiment Hastelloy N Surveillance Specimens - First Group," Oak Ridge National Laboratory, Oak Ridge, TN, 1967.

[10] R. E. Thoma, "Chemical Aspects of MSRE Operations," Oak Ridge National Laboratory, Oak Ridge, TN, 1971.

[11] V. F. Dean, "ICSBEP Guide to the Expression of Uncertainties, Rev. 5," International Criticality Safety Benchmark Evaluation Project, 2008.

[12] E. L. Compere and e. al., "Fission Product Behavior in the Molten Salt Reactor Experiment," Oak Ridge National Laboratory, Oak Ridge, TN, 1975.

[13] R. L. Murray, Nuclear Energy: An Introduction to the Concepts, Systems, and Applications of Nuclear Processes, 6th ed., Oxford, UK: Butterworth Heinemann, 2009.

[14] J. M. Chandler and S. E. Bolt, "Preparation of Enriching Salt 7LiF-233UF4 for Refueling the Molten Salt Reactor," Oak Ridge National Laboratory, Oak Ridge, TN, 1969.

[15] J. R. Engel and B. E. Prince, "The Reactivity Balance in the MSRE," Oak Ridge National Laboratory, Oak Ridge, TN, 1967.

[16] J. R. Lamarsh and A. J. Baratta, Introduction to Nuclear Engineering, 3rd ed., Upper Saddle River, NJ: Pearson, 2012.

[17] P. N. Haubenreich, J. R. Engel, B. E. Prince and H. C. Claiborne, "MSRE Design and Operations Report Part III. Nuclear Analysis," Oak Ridge National Laboratory, Oak Ridge, TN, 1964.